8th ICAAR 1989 KYOTO 8th International Conference on Alkali-Aggregate Reaction

CHARACTERISTICS AND SIMULATION OF CONCRETE CRACKS CAUSED BY AAR

Wataru KOYANAGI*, Keitetsu ROKUGO*, Hiroaki MORIMOTO* and Hiroyuki IWASE*

* Department of Civil Engineering, Gifu University, Yanagido, Gifu 501-11, Japan

1. INTRODUCTION

Concrete cracks caused by alkali aggregate reaction (AAR) relate, more or less, to the mechanical bahavior and safety of structures. Many studies have been made on the subject and there are many reports on the typical crack pattern caused by AAR from qualitative aspect [1,2,3,4]. The present study has two main objects. One is to analyze quantitatively the effect of reinforcement and prestress on the crack characteristics due to AAR. The other is to simulate mathematically the crack occurence and its propagation process with three dimensional finite element method, which will be developed as a diagnosis technique of concrete cracking in the future.

2. CRACK ANALYSIS

Quantitative crack analysis was made for six kinds of reinforced concrete (RC) beam specimens and four kinds of prestressed concrete (PC) specimens. In RC specimens, kinds of concrete and the amount of compression reinforcement were varied. In PC specimens, amount of prestressing force was changed.

As shown in Fig. 1, RC beam specimen had rectangular cross section and its dimensions were 10x18x170 cm. Tensile reinforcement ratio was kept constant at p=1.7% (2D13), while three levels were selected for compression; i.e. p'=0% (none), 0.9% (2D10) and 1.7% (2D13). Two kinds of concrete, normal concrete (NC) and steel fiber reinforced concrete (SFRC), were used. The kinds of RC specimens are listed in Table 1. Yield strength of re-bars of D10 and D13 were 37.1 and 36.0 (kgf/mm^2), respectively. Strength and failure properties of the beams were already reported [2].

The size of the PC prism specimens was 10x10x40cm, which is shown in Fig. 2. Prestressing tendon was a high strength bar (SBPR 122/131) of 19mm in diameter. The bar was arranged at the center of the specimen through a plastic sheath (polyvinyl chloride) with 34mm outer diameter and was held in length by two steel plates of 40mm thick each at both ends of the specimen with nuts. One kind of normal concrete was used. Four levels of induced stresses were chosen, i.e. 0, 20, 40 and 80 kgf/cm^2 and the specimens were named AP-0, AP-20, AP-40 and AP-80, respectively.

Mix proportions of the concretes were about the same where w/c=0.5 and C:S:G = 1:2.1:2.7. For coarse aggrgate as a whole for RC specimens, alkali reactive crushed gravel (bronzite andesite: max. size 20mm) was used and one half of the whole amount was used for PC specimens. In the latter case, the other half of the coarse aggregates was replaced by non-reactive one, because

Table 1 Kinds of RC specimens

Name	Reinf. ratio and position p(%)	d(cm)	p'(%)	d'(cm)
A-1	1.66	15.3	0	
A-2	1.66	15.3	0.93	2.5
A-3	1.66	15.3	1.66	2.7
SA-1	1.66	15.3	0	
SA-2	1.66	15.3	0.93	2.5
SA-3	1.66	15.3	1.66	2.7

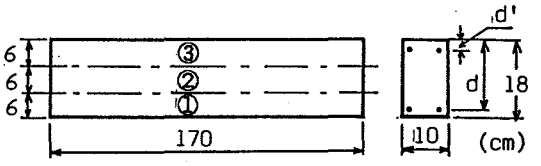

Fig. 1 Size and divisions of RC specimen

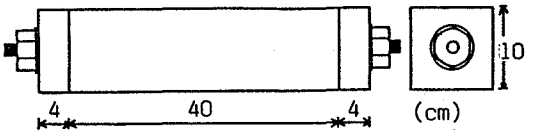

Fig. 2 Shape of PC specimen

the pessimum amount of this gravel was taken into consideration. Non reactive river sand was used. Sodium hydroxide was added to regulate the equivalent sodium oxide content so that it will be 2.3 % of cement content for RC specimens and 3.3 % for PC ones. In case of SFRC, indented steel fibers of 0.5x30 mm (aspect ratio: 60) were added as one volume percent of the concrete.

RC beam specimens were demoulded one day after casting and then stored in a room of 22°C and 80% R.H. for 14 days. Then, the room temperature was raised to 40°C and the specimens were kept under wet condition. PC prism specimens were also treated in the same manner as described above untill 14 days. Then, prescribed amount of prestresses was induced. At the age of 28 days, the stresses were re-induced and then, the room temperature was raised to be 40°C.

Cracks due to AAR were transcribed manually on tracing papers and crack maps were made for each of the opposite sides of every specimen; i.e. totally four maps were made for two specimens under each testing condition. The maps for the analysis were made at the ages of ca. 100 days for PC specimens and ca. 150 days for RC specimens. The maps for RC specimens were optically reduced to one thirds with a copying machine. Cracks on the maps were continuously traced with digitizer, which had an effective trace area of 380x260 mm and resolvability of 1.0 mm. Co-ordinates of the points on the cracks were read and put into a personal computor for every 1.0 mm. Total length of the cracks (CL) as well as the projection length on a beam axis (called as x-axis component, XL, hereafter) and that in a perpendicular direction to the beam axis (called as y-axis component, YL) were calculated for each crack map. The length of a line element for the calculation of components was 1.0 mm. For RC specimens, each map was divided into equally three regions in height as shown in the Fig. 1, and the crack values CL, XL and YL were also obtained for each division.

3. RESULTS AND DISCUSSIONS ON THE CRACK ANALYSIS

Digitized crack data put into the personal computor were reproduced again as crack maps with X-Y plotter. The reproduced maps are shown in Fig. 3 for RC and in Fig. 4 for PC specimens, where one side for each kind of the specimens is shown as an example.

Fig. 5 shows the average total crack length and crack density of one side of the RC specimens. The crack density was defined as the ratio of the total crack length to total area of the specimen. The crack length and density of

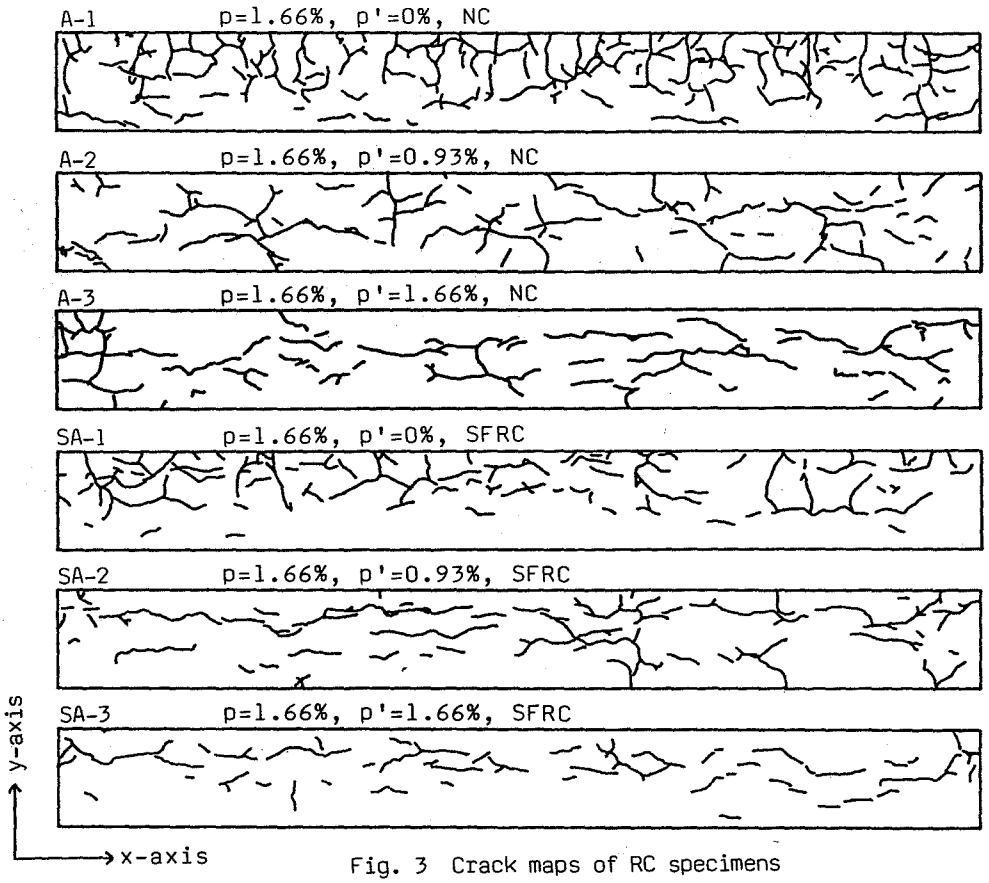

Fig. 3 Crack maps of RC specimens

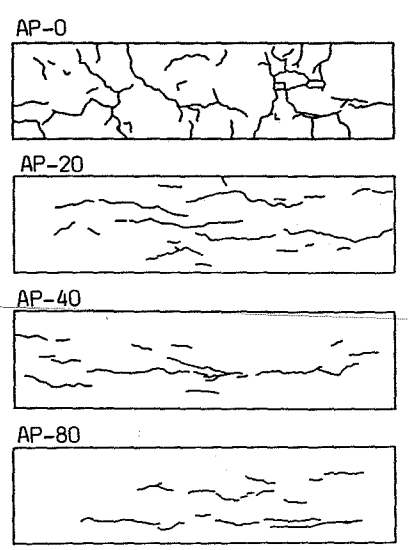

Fig. 4 Crack maps of PC specimens

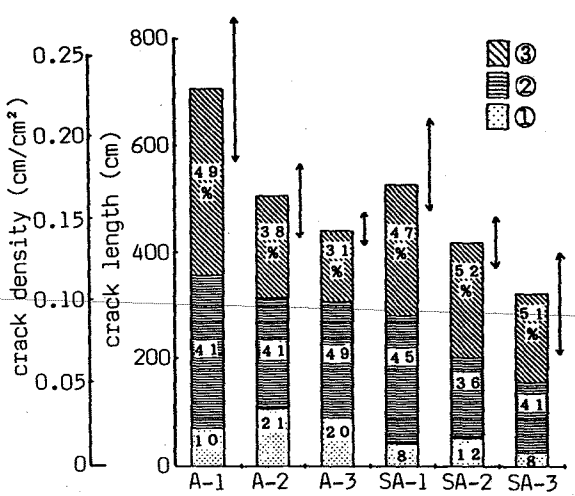

Fig. 5 Crack length and crack density (RC)

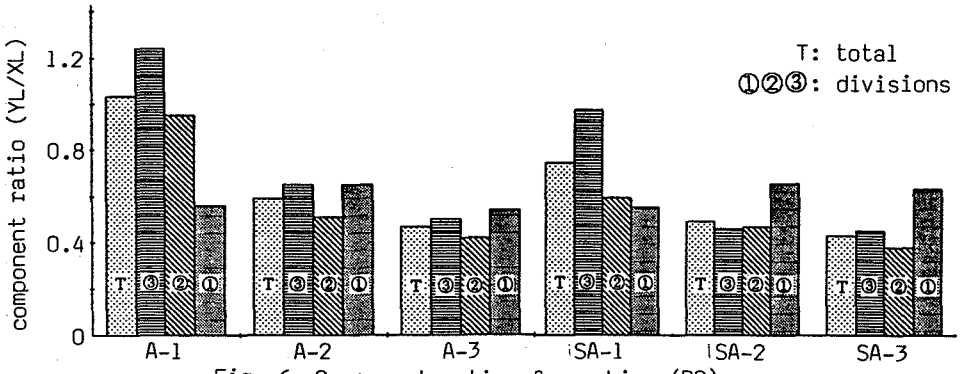

Fig. 6 Component ratio of cracking (RC)

the portion in each division defined in Fig. 1 are also shown in Fig. 5. In addition, the range of measured crack value is shown as an arrow on the right corner of the bar chart of total crack length. In case of RC beam specimens, total crack length decreased as compression reinforcement increased. For normal concrete without steel fibers, the crack lengths in region 1 and 2 changed only slightly when compression reinforcement increased. Only the length in region 3 decreased considerably. In case of SFRC, total crack length and that in each layer were smaller than that of corresponding normal concrete specimen. The maximum crack width was found to be 0.25 mm for A-1 specimen and it was less than 0.1 mm for other specimens.

Fig. 6 shows the ratio of the crack length of y-axis component to that of x-axis component (YL/XL: called as component ratio, hereafter). The component ratio of each of three divisions is also presented at the same time. When the compression reinforcement increased, the y-axis component as well as the component ratio decreased. For example, 1.03 for A-1 specimen and 0.45 for S-3 specimen. Because the reinforcement restrained the occurence of cracks perpendicular to the beam axis, cracks in the beam axis direction became dominant. In the division 3 and 2 of singly reinforced A-1 specimen, the component ratios were 1.24 and 0.95, respectively. The ratio 1.0 means that the cracks occurred quite at random. In the division 1, i.e. in the bottom division, the ratios were less than 0.6 and the cracks occurred mainly in the direction of the beam axis. Except the single reinforcement beams, the component ratio fell between 0.4 to 0.6 and the specimens were restrained as a whole by the reinforcement both in tension and compression. When the reinforcement ratio remained the same, the component ratio became smaller for SFRC. It is most likely that this was caused because the adoption of steel fibers raied the restrained effect of the reinforcement.

Total crack length (CL) and the crack density of PC specimens are shown in Fig. 7. In Fig. 8, the x- and y-component and the component ratio of PC specimens are illustrated. In case of PC specimens, the crack density decreased when the induced prestress increased when the amount of the initial prestress was 40 kgf/cm^2 and less. To the contrary, the total length of the crack, especially that of the x-axis component, increased when the initial prestress increased from 40 to 80 kgf/cm^2. Directions of cracks came to coincide gradually with those of prestressing as the amount of prestress increased. Fig. 9 shows the relation between the expansion and the ages from prestressing. In case of AP-0 and AP-20, specimens expanded with the ages in a hot and humid condition. In case of AP-40 and AP-80, contraction occurred at

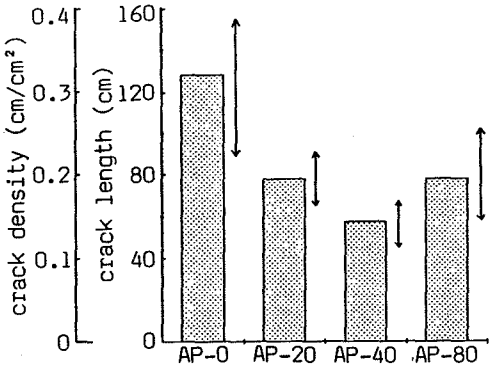

Fig. 7 Crack length and crack density (PC)

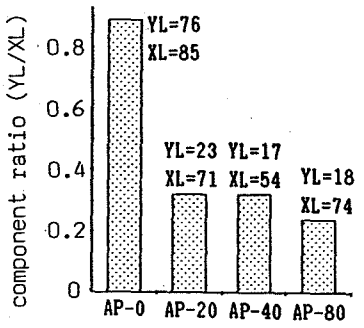

Fig. 8 Component ratio of cracking (PC)

first because creep deformation occurred due to the prestressing. After ca. 40 days, it turned to expand due to AAR. Almost of all the expansion was restrained by prestressing tendon and stress in the specimen raised in addition to the initial stress. This is probably because AP-80 had larger crack length than AP-40 had. The maximum crack width was less than 0.15 mm in any case.

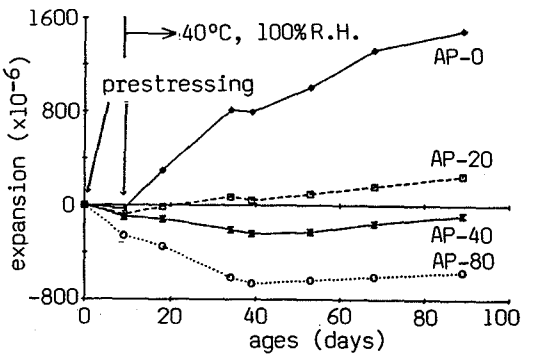

Fig. 9 Expansion of PC specimen

4. SIMULATION ANALYSIS OF CRACKING

Crack initiation and propagation process in concrete due to AAR expansion were simulated with three dimensional FEM (finite element method) analysis [5]. Concrete was modeled as the composition of 64 (4x4x4) elements as shown in Fig. 10. The size of an each element was 5 cm cubic, i.e. the model was 20x20x20 cm. An expansive element, a shaded one, was assumed to be located in the inside of the model concrete. Cracked element was considered to have an orthotropically heterogeneous property in the direction of the cracked surface. In the consitutive equation for the direction in perpendicular to the cracking, tension softening was taken into account. Crack band model was adopted and the tension softening curve was assumed to be straight as shown in the stress strain curve of Fig. 11, where assumed tensile strength and Young's modulus were 30 and 3×10^5 kgf/cm^2, Poisson's ratio was 0.16 and fracture energy G_f was 0.1 kg/cm. The maximum principal strain theory was adopted as a fracture criteria. The expansive element was considered to increase its volume uniformly and continuously, however, in the calculation, the expansion was given stepwise with the increment of 50×10^{-6}. Cracking process on the surface nearest to the expansive element (the front surface) was shown in Fig. 12, where total expansive strain e at each stage is given in the figure. The crack was thought to initiate at the strain of 100×10^{-6} and it did not necessary to agree with the maximum stress point. At the last stage in Fig. 12, the maximum surface strain was ca. 300×10^{-6}. Though it is insufficient in the size of the model and the extent of the calculation, it would be valuable to develop the simulation technique in analyzing the nature of cracking.

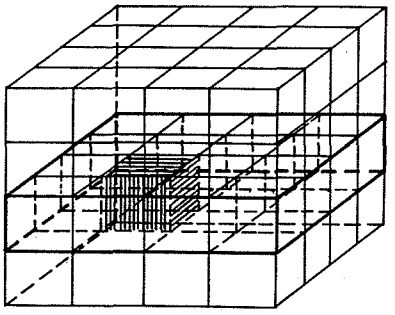

Fig. 10 Concrete model and expansive element

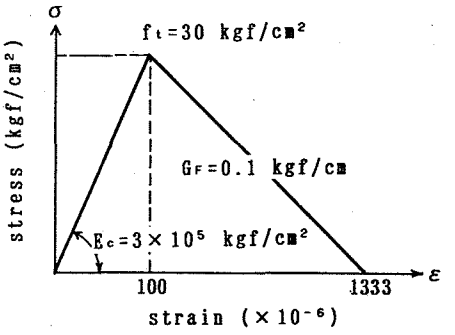

Fig. 11 Tensile stress strain curve

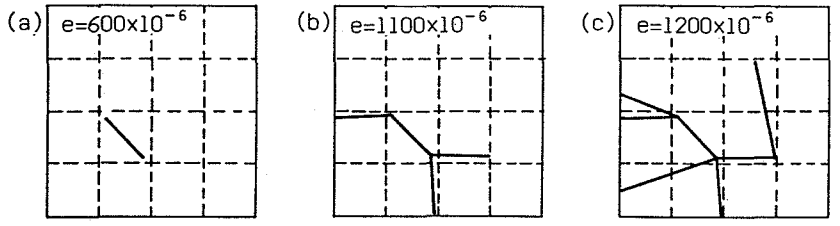

Fig. 12 Cracking process with simulation analysis

5. CONCLUSIONS

The character of concrete cracks caused by AAR was analyzed quantitatively, especially in relation with reinforcement and prestressing. Simulation analysis of crack pattern was also made. Principal conclusions derived are as follows;
(1) In case of RC beam specimens, total crack length and crack component perpendicular to the beam axis decreased when compression reinforcement increased and cracks in the direction of the axis became dominant. Addition of steel fiber also made crack length shorter.
(2) In case of PC specimens, cracks in the stressing direction became dominant gradually when the amount of prestress increased. Crack density decreased with the increase of prestress within 40 kg/cm^2. It increased, however, when the prestress became 80 kg/cm^2.
(3) Cracking process could be simulated, though insufficient, where tension softening was taken into consideration.

6. REFERENCES

[1] Ono, K., Examples of Deteriorations of Concrete Structures due to Alkali Aggregate Reactions, Concrete Journal, 24, 11, 50, 1986.
[2] Koyanagi, W., Rokugo, K. & Ishida, H., Concrete Alkali-Aggregate Reactions (Ed. Grattan-Bellew), 141, Noyes Publications, New Jersey, 1987.
[3] Kobayashi, K., Inoue, S., Yamazaki, T. & Nakano, K., Structural Behaviors of Prestressed Concrete Beams Affected by Alkali-Aggregate Reaction, Proc. Japan Concrete Inst., 9-1, 615, 1987.
[4] Honda, H., Shiraishi, F., Ueda, K. & Hayashi, Y., Influence of Restraint of Steel Bar for Alkali-Aggregate Reaction, Proc. Japan Conc. Inst., 8, 169, 1986.
[5] Morimoto, H. & Koyanagi, W., Study on the Relaxation Analysis of Thermal Stress in Mass Concrete, Proc. Japan Soc. Civil Eng., 402/V-10, 125, 1989.